

## SHORT NOTE

# FINGERPRINT OF OXYGEN VACANCIES IN Gd SUPERCONDUCTORS

H. SHIBAHARA \*, J.P. ZHANG and L.D. MARKS

*Material Research Center, Northwestern University, Evanston, Illinois 60208, USA*

Received 9 August 1988

The arrangement of the oxygen atoms in high temperature superconductors is known to be critical to their properties. High resolution electron microscope imaging (HREM) accompanied by computer simulations has been anticipated to reveal the oxygen vacancies in the basal plane. Although images of sufficient resolution have been reported by many authors, the [100] and [010] projections have not been differentiated experimentally. We confirm here that they are clearly different using a specimen which contains a coherent grain boundary with (100), (001) in one grain parallel to (001), (010) in the second. Unfortunately we find that it is not possible to clearly answer the more important question of the oxygen content at the grain boundary.

## 1. Introduction

It is now well established that oxygen vacancies play a critical role in the superconductivity of the materials  $\text{MBa}_2\text{Cu}_3\text{O}_{7-x}$ , where M is a rare-earth element and the oxygen deficiency can range from 0 to 1; when  $x > 0.5$  the materials are tetragonal and semiconducting, but when  $x < 0.5$  they are, as a rule, superconducting. A question that arose very early in HREM studies of these materials is whether the oxygen vacancies, which are localized in the copper–oxygen basal plane, could be detected. Several authors have mentioned the possibility of detecting the oxygen vacancies by HREM on the basis of image simulations (e.g., refs. [1,2]), but Gibson [3] has raised the ever worrying issue of how well we can interpret experimental images using calculations where there may be experimental ambiguities. To date most HREM analyses have skipped the somewhat tricky issue (e.g., refs. [4–10]).

We have recently been studying the high  $T_c$  superconductor  $\text{GdBa}_2\text{Cu}_3\text{O}_{7-x}$ , in this material focusing primarily on copper-rich planar defects [9,10]. In this sample we found, by chance, a

coherent grain boundary with the two grains on either side oriented along [100] and [010]. This presents the “ideal” specimen where we can precisely compare the two zones for identical thicknesses and defoci without most of the uncertainties common to HREM. We conclude from our analysis that we can definitely differentiate between the two. What we cannot as yet do, unfortunately, is determine the oxygen content at the grain boundary in sufficient detail to permit modeling of its electrical characteristics.

## 2. Experimental method

A sample of composition  $\text{GdBa}_2\text{Cu}_3\text{O}_{7-x}$  (see ref. [10] for details), prepared by the solid state reaction of hyperpure gadolinium oxide, barium oxide and cupric oxide, was crushed gently by two glass plates to prevent mechanical deformation. The specimens were then mounted on holey carbon films and examined in a Hitachi H-9000 operated at 300 kV with a spatial resolution of better than 0.18 nm. Image simulations using the NUMIS programs written at Northwestern University were carried out on an Apollo 660 workstation. The lattice parameters of the bulk specimen were measured by the X-ray powder diffraction method and

\* Present address: Kyoto University of Education, Fushimiku, Kyoto 612, Japan.

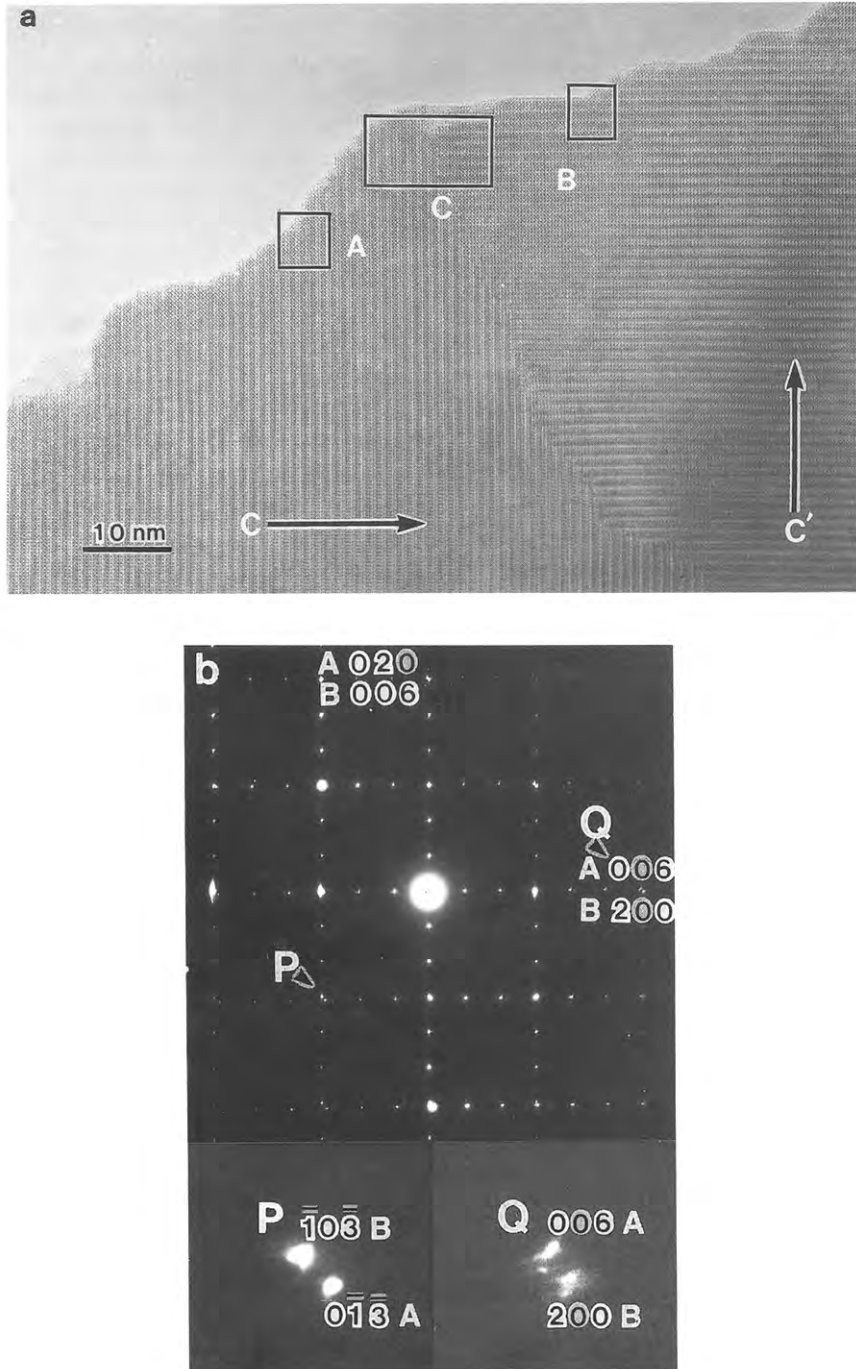


Fig. 1. (a) Image showing two grains with the  $c$ -axes normal to each other connected by a coherent grain boundary; note the difference in the image contrast in the thin regions near the surface. (b) Selected area diffraction pattern from the same region with enlargements of spots P and Q. In (a) some spurious fine detail is due to moiré fringes from the screen printing.

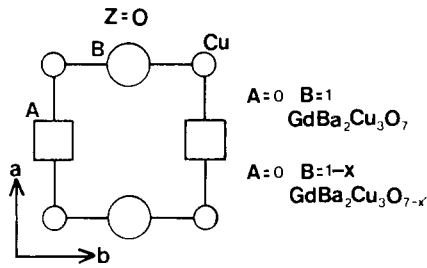


Fig. 2. Diagram of the atomic arrangement on the basal plane. Note two kinds of chains of Cu-O along the *a*-axis and Cu-O vacancies along the *b*-axis.

refined by a least-squares method using an internal NBS Si standard – see ref. [10].

### 3. Results

Fig. 1a shows an image of two adjacent grains with the *c*-axes normal to each other, the zone axes being [100] and [010], with the selected area electron diffraction pattern which indicates the orientations of the two grains shown in Figure 1b. Theoretically, such a coherent grain boundary or twin indicates a disorder-order transformation from a cubic perovskite at high temperature to an orthorhombic structure at lower temperature as for YBa<sub>2</sub>Cu<sub>3</sub>O<sub>7</sub> [4]. The orientation domains will arise due to the loss of the 3-fold symmetry of the cubic perovskite [11].

It should be noticed that even in very thin regions a slight difference in the image contrast can be detected, for example the areas A and B of

fig. 1a. The enlargements of the diffraction spots P and Q in fig. 1b along [100] and [010] shows the expected splitting. From the diffraction pattern of fig. 1b the ratio along two axes of *c*/3 to *a* and *c*/3 to *b* were measured to be 1.016 and 1.002 respectively, which is close to the calculated values of 1.013 and 1.001 respectively, based upon the results of X-ray diffraction [10]. The coherent boundary between the two grains can be considered as a twin boundary (albeit without a mirror plane symmetry), and the splitting of the diffraction spots at P can be interpreted as the result of this twinning. A schematic diagram of the atomic arrangement of the basal plane derived from X-ray powder diffraction is shown in fig. 2 for reference.

Ourmazd and Spence [1] and Huxford et al. [2] reported that the difference in image contrast between [100] and [010] projections can only be observed in thicker regions, for example in the Y-based compound, thicker than 10nm. However, fig. 1a shows apparently different contrast in the two regions A and B. In order to discuss this, the change in amplitude of several of the main waves as a function of the specimen thickness is shown in fig. 3. This indicates that even at small thicknesses it should be possible to discriminate between the two projections; for instance, the (002) beam is far stronger for the [010] orientation where there is also an extinction of the (003) reflection at about 3.7 nm as arrowed. Calculations were carried out around the potentially good thickness of 3.7 nm, for *C<sub>s</sub>* = 0.9 mm, an accelerating voltage of 300 kV, a focal spread of 8 nm and a convergence

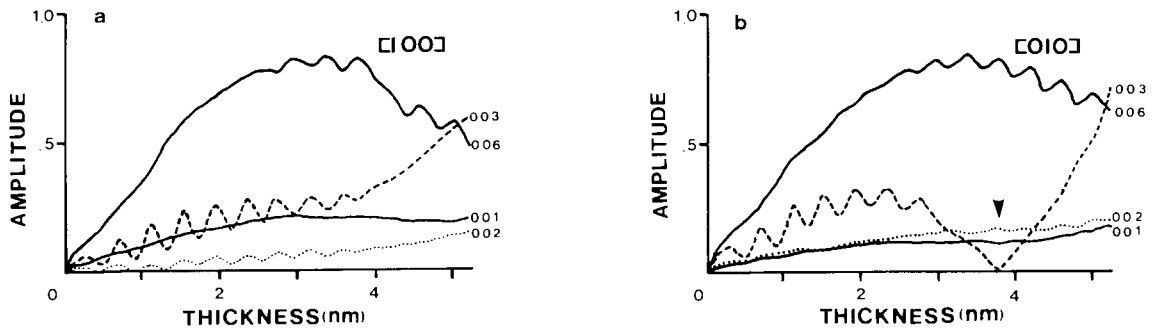


Fig. 3. Amplitude of the main diffracted beams as a function of thickness for the [100] and [010] projections. The arrow in (b) indicates the thickness of 3.7 nm used for the calculations in figs. 4, 5b and 6.

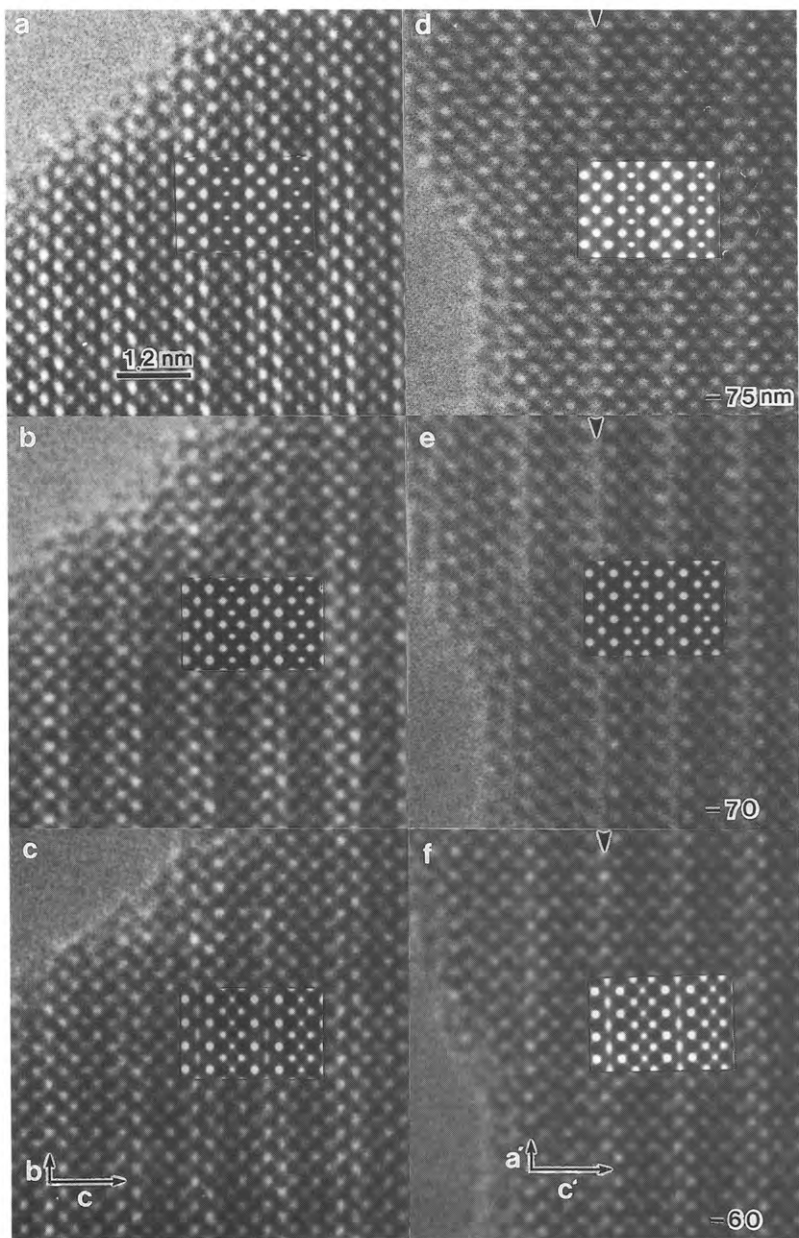


Fig. 4. Through-focus images for [100] and [010], taken from the regions A and B in fig. 1a. Inset are the calculated images for thickness of 3.7 nm,  $C_s = 0.9$  mm, 300 kV, focal spread of 8 nm and convergence of 1.0 mrad. In the images along [010] (d, e and f), the basal plane appears substantially lighter.

of 1.0 mrad. Huxford et al. [2] pointed out that the Debye–Waller factors can have an effect on the images. However, at the thicknesses used here we found by comparing simulations with different

temperature factors that this was not important. Fig. 4 shows a comparison of observed and calculated images, with fairly good agreement with the experimental results. (Figs. 4d–4f are rotated by

90° for comparison.) Apparent in figs. 4d, 4e and 4f is bright contrast indicated by arrows in the basal plane for the [010] direction which is a fairly clear-cut characteristic of this zone.

Assuming that the boundary between the two grains is almost parallel to the incident electron beam and that the two grains are completely coherent (i.e. neglecting the local strain field), the

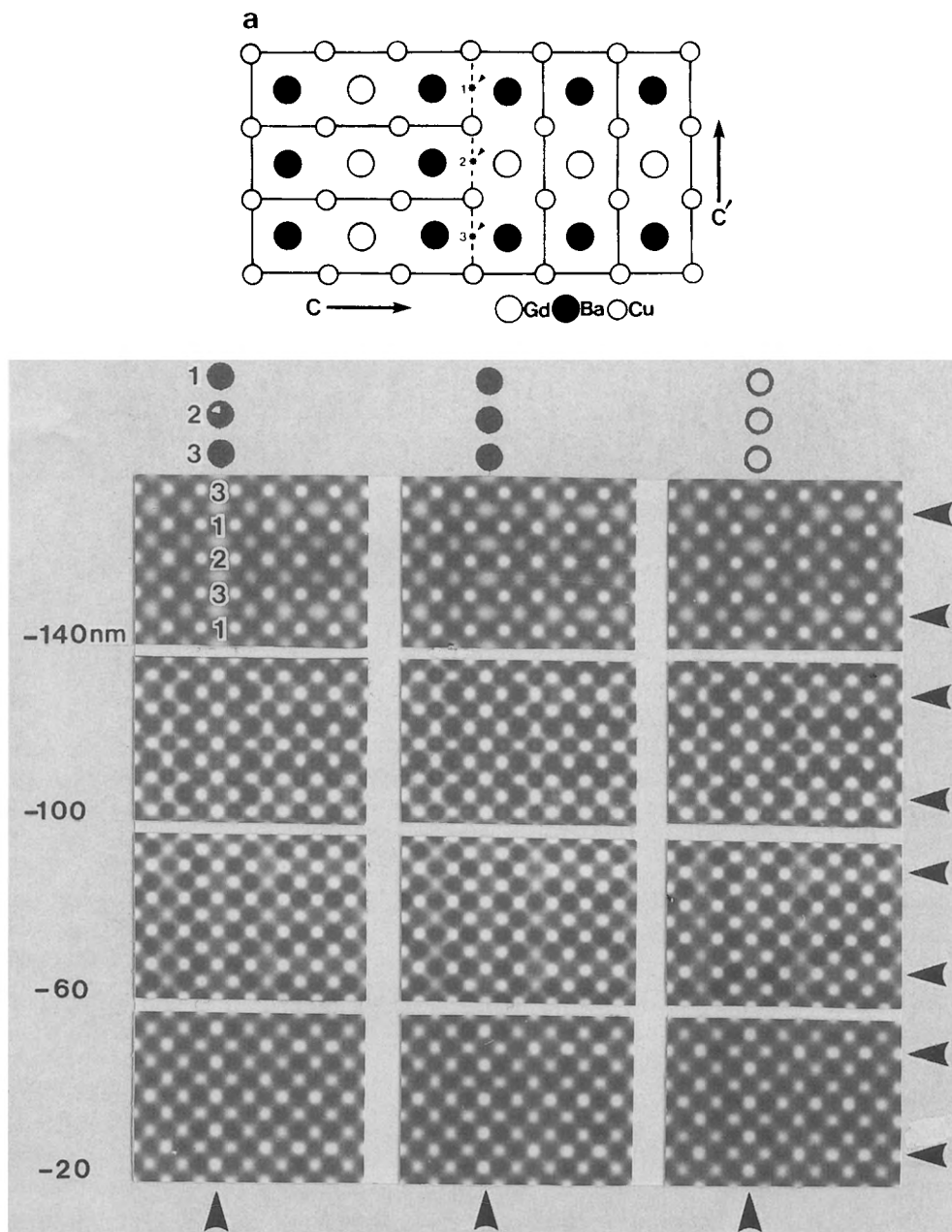


Fig. 5. (a) Structure model of the coherent grain boundary; arrows indicate possible positions of oxygen atoms in the grain boundary. (b) Calculated results for three different occupancies of the oxygen sites: on the left full occupancy of sites 1 and 3 as marked in the figure and 0.6 occupancy of site 2; in the center full occupancy of all three sites and on the right no occupancy of any of the sites; the image contrast was not substantially affected by the oxygen atoms in the boundary layer.

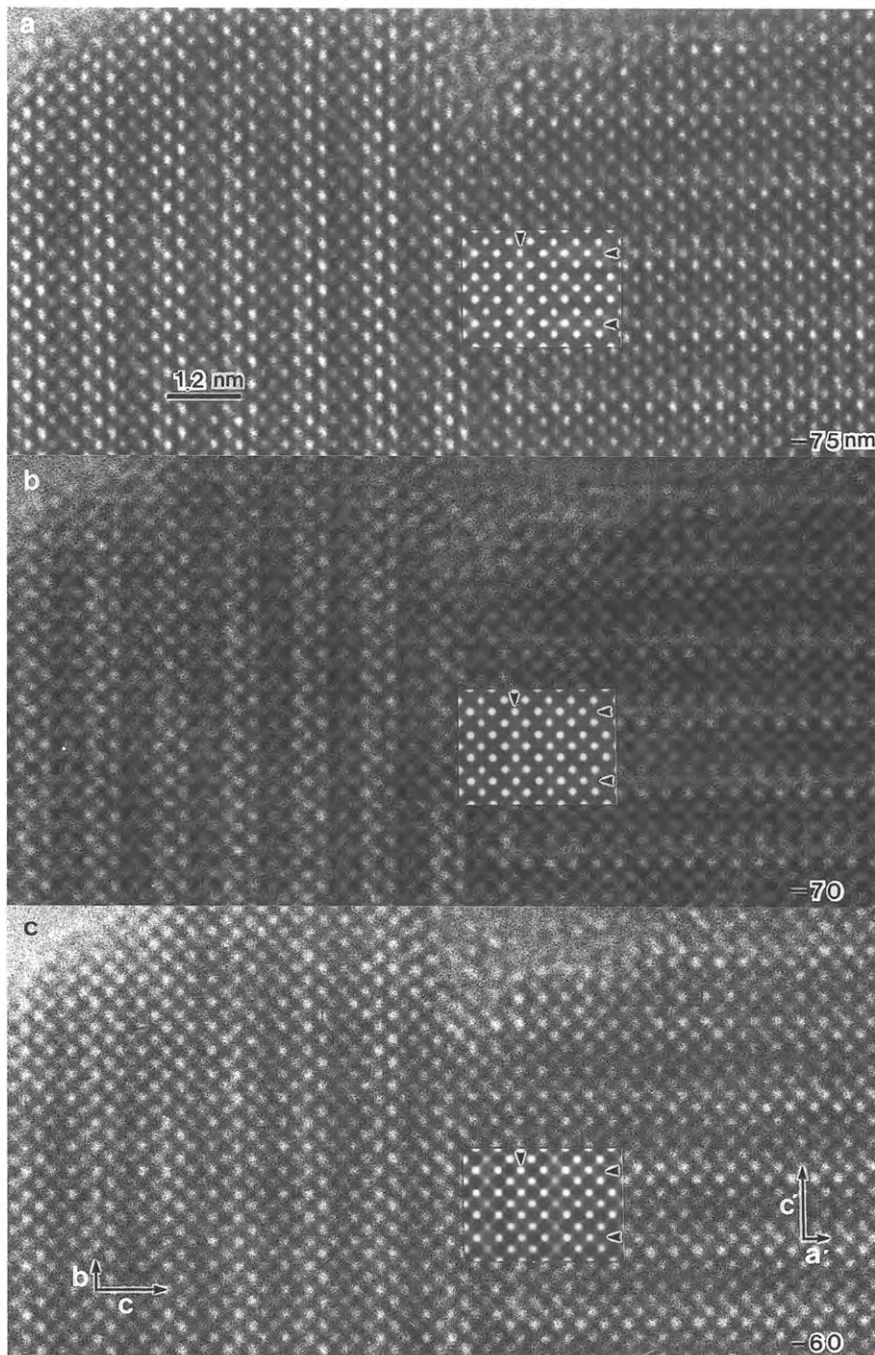


Fig. 6. Through-focus images of the coherent grain boundary taken from the region marked C in fig. 1a. Calculated results on the basis of the structure model in fig. 5a are inset.

atomic arrangement of the cations at the boundary marked C in fig. 1a can be deduced from the images without any difficulty. A structure model

for the grain boundary is shown in fig. 5a. In order to examine the arrangement of the oxygen atoms in the boundary, image calculations were

carried out for several structure models which differ in the oxygen occupancies in the boundary layer at the sites 1–3 marked in fig. 5a. Fig. 5b shows the calculated results for a thickness of 3.7 nm, defocus values of  $-140$ ,  $-100$ ,  $-60$  and  $-20$  nm with varying oxygen content in the boundary. In fig. 5b there was no clear difference in the calculated image contrast as a function of the oxygen content. Experimental through-focus images of the grain boundary corresponding to the region of the framework of C in fig. 1a are shown in fig. 6 together with the calculated images for defoci of  $-75$ ,  $-70$  and  $-60$  nm.

#### 4. Discussion

We have demonstrated here that one can differentiate between oxygen sites even in thin regions of a material such as a superconductor. One factor which has clearly helped in this is that we do not have any amorphous contaminants on the surface which would include pseudo-noise obscuring fine detail in the image. This is due to the use of turbomolecular pumping of the objective area, rather than diffusion pump. Some other important points are the use of gentle crushing to minimize mechanical deformation, the use of relatively low beam currents so as not to grow amorphous material on the surface by radiation damage [9], and the use of a focal series rather than just one “optimum defocus” image. In some respects it is a little depressing that the calculated images indicate that we cannot determine the oxygen content at the boundary itself, which would be a more notable result. With the ever increasing use of direct digitization techniques, it may be possible to detect and quantify the small image changes due to such phenomena in the future.

#### 5. Conclusions

Using a coherent grain boundary we have experimentally demonstrated that the  $[100]$  and  $[010]$  projections of  $\text{GdBa}_2\text{Cu}_3\text{O}_{7-x}$  can be differentiated. The cation positions at the grain boundary can be determined by careful comparison with image simulations, but the oxygen occupancy could not be.

#### Acknowledgment

This work was supported by the National Science Foundation through the Northwestern University Materials Research Center on Grant no. DMR 85-20280

#### References

- [1] A. Ourmazd and J.C.H. Spence, *Nature* 329 (1987) 425.
- [2] N.P. Huxford, D.J. Eaglesham and C.J. Humphreys, *Nature* 329 (1987) 812.
- [3] J.M. Gibson, *Nature* 329 (1987) 763.
- [4] L.D. Marks, J.P. Zhang, S.-J. Hwu and K.R. Poeppelmeier, *J. Solid State Chem.* 69 (1987) 189.
- [5] H.W. Zandbergen, G. Van Tendeloo, T. Okabe and S. Amelinckx, *Phys. Status Solidi* 103 (1987) 45.
- [6] K. Hiraga, D. Shindo, M. Hirabayashi, M. Kikuchi and Y. Syono, *J. Electron Microsc.* 36 (1987) 261.
- [7] Y. Matui, S. Takekawa and N. Iyi, *Japan. J. Appl. Phys.* 26 No.10 (1987) L1693.
- [8] W. Krakow and T.M. Shaw, *J. Electron Microsc. Tech.* 8 (1988) 273.
- [9] L.D. Marks, D.J. Li, H. Shibahara and J.P. Zhang, *J. Electron Microsc. Tech.* 8 (1988) 297.
- [10] H. Shibahara, S.-J. Hwu, K.R. Poeppelmeier and L.D. Marks, *J. Solid State Chem.*, submitted.
- [11] G. Van Tendeloo and S. Amelinckx, *Acta Cryst.* A30 (1974) 431.